A comparison of strategies to extend the operating range of radial compressors for turbocharging

Carlo Cravero and *Davide* Marsano*

Dipartimento di Ingegneria Meccanica, Energetica, Gestionale e dei Trasporti, Università di Genova, Genoa, Italy

Abstract. The operating range extension of radial compressors is a crucial aspect in turbocharging the internal combustion engines in order to extend the operating range of the system at high efficiency for fuel and environmental impact reduction. The future scenario of automotive propulsion will have the fuel cells at the top of the ranking of possible reference systems in substitution of thermal reciprocating engines. Proton exchange membrane fuel cells for automotive or aerospace vehicles are frequently turbocharged because compressed air for the fuel cell stack is required in the cathode system. Therefore, like in turbocharged internal combustion engines, a radial compressor is combined and connected with a radial turbine to exploit the thermal energy of the exhaust gas from the fuel cell. The study and the development of this sort of radial turbomachinery is still strategic to guarantee high performance of the overall propulsion system. The operating range is an important issue and current turbocharger design must be adapted to the new requirements of the fuel cells systems with a need for extending it. Various techniques to extend the operating range of the centrifugal compressor have been investigated and a summary is reported in this work, with a focus on the casing treatment. Through a CFD simulation campaign with appropriate simplified models, the effects of installing the ported shroud, the shutter or the axial groove have been calculated with respect to a baseline configuration. These simulations have supported the identification of the main limits and advantages for each of these solutions at different operating regimes. The performance maps and some physical parameters of interest have been compared.

1 Introduction

In the next decade, a strong development in the automotive propulsion industry will be necessary to replace the traditional thermal reciprocating engines as required by the new European regulations [1]. One of the selected solutions concerns fuel cells, which can be close to “nearly” zero emissions vehicles, with a high efficiency and quick response. The performance of the fuel cell plant can be further increased through the use of pressurized air system to obtain a higher power density [2,3]. In a PEM fuel cell hydrogen and oxygen react

* Corresponding author: davide.marsano@edu.unige.it

© The Authors, published by EDP Sciences. This is an open access article distributed under the terms of the Creative Commons Attribution License 4.0 (https://creativecommons.org/licenses/by/4.0/).

electro-chemically providing water as a waste product. At the cathode the installation of a compressor, an electric engine and a turbine connected on the same shaft by the turbocharger are required. The centrifugal compressor is the preferred solution because of its specific speed, small size, low weight, quick response, long life and high efficiency [4-6]. According to Venturi et al. [7] the turbocharger is the most expensive subsystem of the fuel cell cathode part requiring the highest power demand. Also an electric motor is necessary because the radial turbine can only provide about 1/3 of the required power by the compressor. For this reason, the centrifugal compressor must be designed to optimize performance in terms of pressure ratio and efficiency. A further design target consists in extending the operating range in order to guarantee a sufficient stability margin for all operating conditions [8]. In fact, the operating range is limited by two distinct phenomena: chocking at high flow rates and surge at low ones. The latter induces strong fluctuations in the flow structure that can cause vibrations with damage to the compressor and to the entire system; this condition must be avoided and design strategies to obtain a large surge margin are needed.

Numerous studies have focused on the understanding of unsteady three-dimensional flow to develop strategies aimed at extending the surge margin, Flow phenomena like stall and rotating stall in the centrifugal stage subcomponents typically occur before the stability limit. Iwakiri et al [9] and Tomita [10] have investigated the impeller stall; they highlighted the vortical structure consisting of a tornado-type separation vortex caused by full blade separation at leading edge. Similar conditions for the vaned diffuser have been found by Everitt [11] and Liu [12]. In vaneless diffuser, the reverse flow from the casing is caused by the development of the boundary layer separation [13]. The matching of a correct volute plays a key role on the development of unstable phenomena especially at high speeds [14]. There are two main strategies to extend the surge limit in centrifugal compressors: active or passive flow control devices. Active methods use actuation devices including the variable inlet guide vanes [15,16]. Passive methods induce changes in the flow structure, like the casing treatment family: the ported shroud, the inducer casing bleed system, internal recirculation or ring groove arrangements and shutter. The ported shroud is an axisymmetric cavity that connects a portion of the impeller with the adduction duct; it reduces the low momentum flow, which in the inducer region at low mass flow rate would partially obstruct it, forcing it to be recirculated into the cavity. With the above strategy, the surge condition can be shifted to a lower mass flow. On the other hand, the performance can decrease for certain conditions. Several researchers have analysed and optimized the geometry of this device [17-19]. Other authors believe it is more effective to install appropriate vanes into the cavity to control the recirculation flow in order to achieve significant surge margin improvement [20-22]. The axial groove consists of a similar solution to the previous but more compact: there is a single opening on the inducer shroud where grooves are designed to guide recirculating flow with minimum losses. The benefits of axial grooves has been studied is numerical works [23,24]. Finally, circumferential grooves can be installed at the diffuser to alleviate blockage in vaned diffusers [25,26]. Nowadays, CFD techniques are increasingly used for the design and fluid-dynamic analysis of turbomachinery with three dimensional models which can be also integrated into design strategies [27] or used to understand the complex flow structures toward surge with unsteady analysis [28]. At the limiting operating condition a complete surge cycle [29] can be simulated for a centrifugal compressor stage. In previous works, the authors have developed different criteria to predict the limit mass flow rate at surge conditions by using a simple and efficient CFD 3D approach during the design and development phase of a compressor stage. Both vaned [29] and vaneless diffusers [30,31] have been considered. The flow angle criterion at the diffuser exit has been also demonstrated on a compressor with the ported shroud [32]. Similar CFD models can be used also for more complex cases like a two-stage radial compressor for air conditioning [33] or for aero-acoustical tonal noise prediction [34]. On the experimental side, the vibrational analysis can

be effectively used as surge precursor [35-37]. In this work, a centrifugal compressor stage, equipped with various device to extend the surge margin, is studied with a CFD model in order to be understand the effects on performance and on the extension of the operating range of the different casing treatment solutions. In addition to the baseline configuration, the ported shroud and the axial groove cases have been simulated. After having quantified the advantages or disadvantages of these solutions, the flow mechanism induced by these devices are described. The effect of the shutter addition at the lowest rotational speed has been also evaluated.

2 Case study

A small size centrifugal compressor for turbocharging applications is the reference configuration for the study. The compressor data is proprietary and covered by a non-disclosure agreement therefore the geometric data is provided in non-dimensional form with respect to the inlet diffuser radius and numerical data is expressed in corrected form (referred to the corresponding design value) or omitted. The rotor is equipped with six main blades and six splitter blades, which are backswept and the diffuser is vaneless. Table 1 reports the main geometric data of the configuration.

Table 1. Geometrical non-dimensional data of the reference compressor.

Geometrical parameter	Value
Impeller blade number	6+6
Span at diffuser inlet	0.0706
Radius at rotor leading edge hub	0.1755
Radius at rotor leading edge tip	0.7166
Radius at diffuser outlet	1.5323
Maximum radius of the volute	2.3519

The passive devices for the extension of the operating range have been integrated into the baseline case. In Figure 1 the compressor sketches with the different devices mounted for the casing treatment are shown.

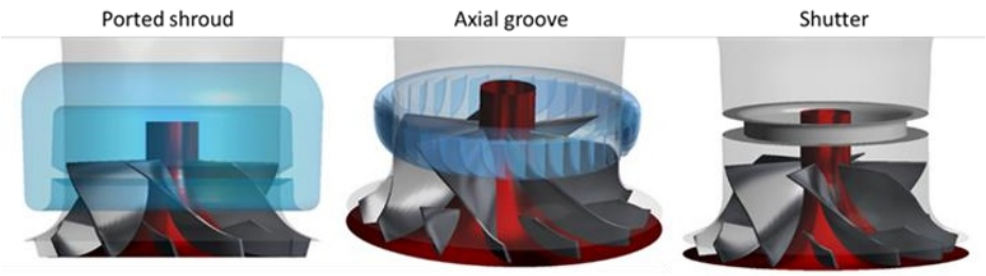

Fig. 1. 3D views of the compressor with the passive devices for the casing treatment.

3 Methodology

The commercial Ansys CFX software was used to solve the RANS equations. The CFD simulations were carried out using preferably the so-called “Simple model”. The simple model was designed to be efficient from a computational point of view to be routinely used in the design phase or to simulate the performance maps in a large dataset of operating

conditions. It has been already validated in previous research activities [28,29] and extensively used for practical applications. It consists of a sector of the adduction channel, a single impeller channel (with a main blade and splitter blade) and a single diffuser channel with a convergent duct for stability reasons. The additional devices were added with an angular portion equal to that of the stage (60° from the number of main blades).

The stage has been discretized with Ansys Turbogrid software using a structured mesh with hexahedral elements using the ATM optimized topology. The ported shroud and the axial grooves have been meshed with an unstructured grid using ICEM CFD from the Ansys CFD platform. If the shutter is present, also the intake domain has been discretized with an unstructured grid. Special attention was given to the grid clustering at the walls of each component, in order to ensure a Y+ value lower than unity. At least 48 cells in the blade spanwise direction were used to model the blade with a tip clearance gap. Ten prismatic layers were created in the unstructured grids to solve the boundary layer; a cell size range between 2.0 and 0.1 mm in high curvature regions was used for the tetrahedral elements. The global mesh of the stage consists of about 2.3 million cells: 0.33 Mcells for the inlet duct, 1.4 Mcells for impeller, and 0.6 Mcells for the diffuser. Concerning the unstructured grid blocks: 1.05 Mcells for the ported shroud, 2.0 Mcells and 0.8 Mcells for the intake in the case with shutter. The mesh sensitivity analysis was carried out to select the mesh that predicts a performance variation less than 1% with respect to finer meshes. This sensitivity analysis was performed using the mesh parameters used in previous works for the compressor stage [28–32]. The turbulence model adopted is the k- ω SST, which is a combination of the k-ε and k-ω turbulence models; the former model is used for the free stream flow and the latter is used for modelling near wall turbulence. The total energy model was activated to solve the energy equation written in terms of enthalpy. The fluid (air) is treated as a perfect gas. The following boundary conditions were imposed: at the inlet the total pressure, the total temperature and a turbulence intensity of 5% were set, at the outlet the mass flow rate condition was set, except for the near choking conditions where the static pressure was used. The intake and the impeller have a uniform rotational speed with the interface between the two domains as a fluid-fluid GGI. The frozen rotor option with a specified pitch angle of 60°–60° has been set for the interfaces impeller-diffuser and stage-ported shroud or stage-axial groove. For the devices coupled with the rotating domain, the option “not-overlap” is set to specify the counter-rotating condition for the impeller shroud. The periodicity condition was set on the side surfaces of the stage and of the ported shroud or axial groove portion, while the remaining walls were set as adiabatic no-slip, with the exception of the upstream hub, which was set as an inviscid wall. The walls of the shutter have been set as counter rotating no-slip wall. All the equations were solved with second order numerical schemes and steady simulations were performed using this model. This numerical model has been previously validated by comparing experimental data [28-32].

The performance of the compressor is evaluated with the pressure ratio and isentropic total-to-total efficiency from the inlet adduction duct and the diffuser outlet according the (Eq. 1-2):

$$\beta_{tt} = \frac{P_{t,ou}}{P_{t,in}} \tag{1}$$

$$\eta_{tt} = \frac{(P_{t,ou}/P_{t,in})^{(k-1)/k} - 1}{(T_{t,ou}/T_{t,in}) - 1} \tag{2}$$

4 Results

The performance of the baseline centrifugal compressor has been compared to those obtained with the additional passive devices. Figure 2 shows how the pressure ratio and efficiency curves are affected for the three passive strategies; two reference rotational (non-dimensional) speed values, design and high speed, are considered. The limiting stable point in the operating range has been determined through the use of a stability criterion, previously developed by the authors [30,31].

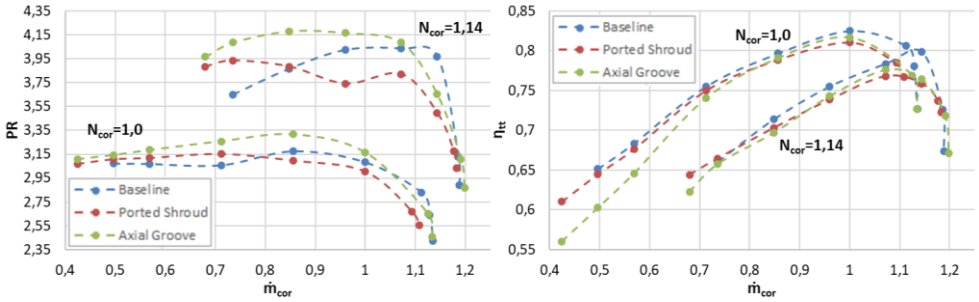

Fig. 2. Comparison of the performance maps for the configurations baseline, with ported shroud and with axial groove: (at left) pressure ratio; (at right) isentropic total-to-total efficiency.

It can be observed that both devices lead to an increase of the pressure ratio towards the lower massflow rate; this improvement is higher at the highest iso-speed. Furthermore, the axial groove brings greater benefits; the pressure curve is always higher than the one with the ported shroud. In terms of efficiency it can be observed that the baseline configuration has the best values, with the exception of near surge conditions at N_{cor}=1.14 and the lowest values are found with the axial groove. However, the main advantage of both casing treatment techniques is to increase the surge margin by 11% for the design iso-speed and 12% for the highest. On the other hand, a slight reduction in the maximum massflow rate is observed only in the case with the ported shroud.

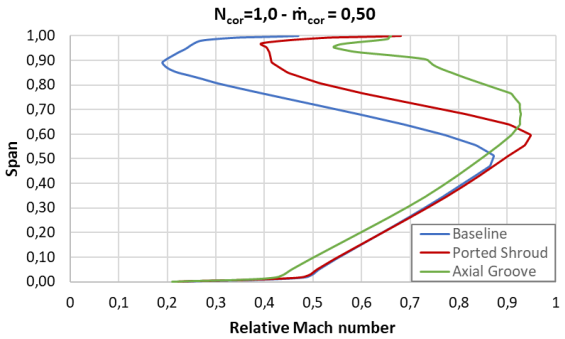

Fig. 3. Comparison of the hub-to-shroud distribution of the relative Mach number at the leading edge for the different compressor configurations, at near surge condition.

To understand the underlying fluid dynamic mechanisms that make these techniques effective a deep post processing of the results has been performed. As an example, Figure 3 shows the hub-to-shroud distributions of the (circumferentially averaged) relative Mach at the rotor leading edge, for a near surge condition, at the design iso-speed. When a compressor operates at the lowest flow rates, a low momentum zone is generated on the shroud, which

extends over an increasingly large portion of the channel reducing the effective blade section [30]. At the same operating condition, it can be observed that at the leading edge both devices reduce the entity of this low energy flow. The axial groove allows almost the entire blade to work properly. The operating principle of the ported shroud is to recirculate the low momentum flow from downstream by reintroducing it into an upstream area where it mixes with the main flow causing a re-energization that creates a higher relative Mach near the blade tip [32]. The axial groove works in a similar way, but there are a certain number of grooves with a single port on the shroud, it directly "cleans" the inducer region by dragging the low momentum flow and releasing it further upstream. The grooves are designed to force a tangential velocity component on the recirculating flow, so it mixes with the main flow, by generating a more suitable flow incidence at the rotor leading edge. However, these mixing with both devices leads to mixing losses which lower the efficiency. With the axial groove, the flow guided by the inclination of the grooves suffers greater losses. Both configurations are advantageous towards the surge, rather than at higher flow rates, because the recirculation into these devices is more effective, from design purposes, at low mass flow rates. This can be seen in Figure 4 where the absolute Mach contour has been reported in a middle plane for two operating conditions. It is evident that at lower massflow rate the flow is more organized with a better fill of the grooves without large stagnation zones (blue colours). On the other hand, at higher massflow rates, where there is no low momentum region in the main channel to be drawn, their function is lost, causing an undesired reduction in flow incidence with the reduced portion of the recirculating fluid in the two devices.

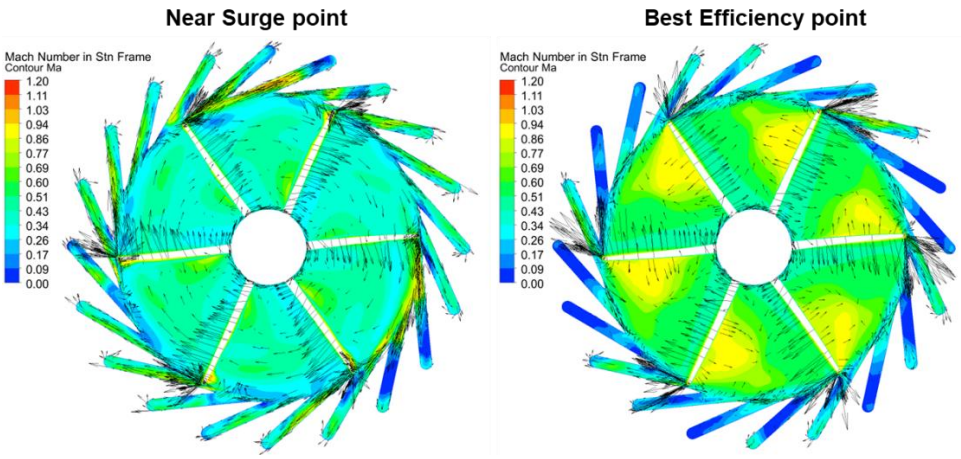

Fig. 4. Comparison of the absolute Mach contours in a middle plane of axial grooves, for different operating conditions.

For the lower iso-speed, where the phenomenon of the flow separations and the low momentum area have an more marked impact on the stage, due to the lower energy in the main stream, the adoption of the shutter has been evaluated. Figure 5 shows the pressure ratio and efficiency trends at low rotational speeds for the baseline configurations and with shutter.

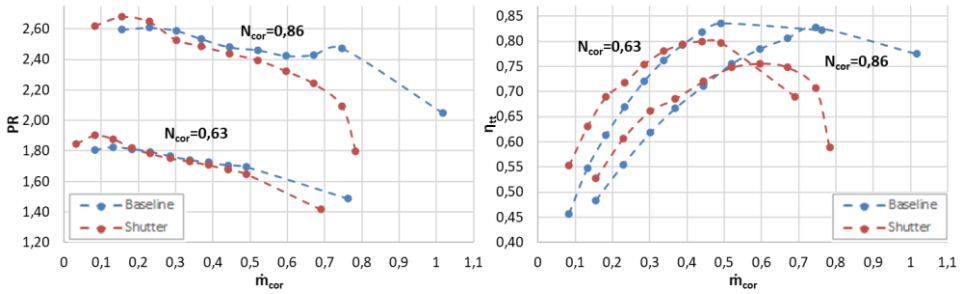

Fig. 5. Comparison of performance maps for baseline and with shutter configurations at low rotational speed

It can be observed that the shutter leads to an improvement both for pressure ratio and for the efficiency. Its operating principle is to narrow the channel on the shroud before of the leading edge to accelerate the flow and to reorganize its structure to counteract the formation of the low momentum region on the blade tip. However, this solution is less effective by increasing the rotational speed, because the main flow normally gradually recovers a higher energy without the need for a reduced passage section. Moreover, the shutter anticipates the chocking phenomenon by lowering the maximum attainable massflow rate; the sonic conditions area reached before with a smaller flow passage at higher speeds.

5 Conclusions

A simplified CFD model of a centrifugal compressor has been used and integrated with ported shroud, axial groove or shutter in order to evaluate their effects on performance and on the extension of the operating range. Wider operating range of about 10% for the ported shroud and axial grooves have been detected. The latter device offers a more compact solution (lighter and less expensive) and it leads to a more marked increase of the pressure ratio at lower massflow rates by increasing the rotational speed. A comparison of the flow structure at the leading edge has highlighted the reduction of the low momentum zone at the inducer in the various configurations. However, both devices give an efficiency reduction due to mixing losses. At low rotational speeds, the introduction of the shutter has been found beneficial but with high rotational speed, the performance benefits are reduced with a lower chocked mass flow.

References

1. Regulation of the UE parliament and Council 2021/0197 (COD): COM(2021) 556 final.
2. J. M. Cunningham, M. A. Hoffman, D. J. Friedman, *A Comparison of High-Pressure and Low-Pressure Operation of PEM Fuel Cell Systems*, SAE 2001 World Congress, Detroit, 2001-01-0538 (2001)
3. W. K. Galen, A. H. Myron, *A Comparison of Two Air Compressors for PEM Fuel Cell Systems*, Virginia: Virginia Polytechnic Institute and State University (2001)
4. B. Blunier, A. Miraoui, *Proton exchange membrane fuel cell air management in automotive applications*, Journal of Fuel Cell Science and Technology, 7, 4, p. 727 (2010)

5. C. Bao, M. Ouyang, B. Yi, *Modeling and optimization of the air system in polymer exchange membrane fuel cell systems*, Journal of Power Sources, 156, 2, pp. 232–243 (2006)
6. A. Kerviel, A. Pesyridis, A. Mohammed, D. Chalet, *An evaluation of turbocharging and supercharging options for high-efficiency fuel cell electric vehicles*, Applied Sciences, 8, 12, p. 2474 (2018)
7. M. Venturi, J. Sang, A. Knoop, G. Hornburg, *Air supply system for automotive fuel cell application, In SAE Technical Paper Series*, SAE International (2012)
8. S. Lück, M. Schödel, M. Menze, J. Göing, J. R. Seume, J. Friedrichs, *Impact of Compressor and Turbine Operating Range Extension on the Performance of an Electric Turbocharger for Fuel Cell Applications*, In Turbo Expo: Power for Land, Sea, and Air, Vol. 86052, p. V007T18A020 (2022)
9. K. Iwakiri, M. Furukawa, S. Ibaraki, I. Tomita, *Unsteady and Three-dimensional Flow Phenomena in a Transonic Centrifugal Compressor Impeller at Rotating Stall*, Proceedings of ASME Turbo Expo 2009, GT2009-59516 (2009)
10. I. Tomita, S. Ibaraki, M. Furukawa, K. Yamada, *The Effect of Tip Leakage Vortex for Operating Range Enhancement of Centrifugal Compressor*, ASME Journal of Turbomachinery, Vol.135, No.3, 051020 (2013)
11. J. N. Everitt, Z. S. Spakovszky, *An investigation of stall inception in Centrifugal compressor vaned diffuser*, ASME J. of Turbomachinery, Vol 135, 011025-1 – 10 (2013)
12. Y. Liu, B. Liu, *Investigation of unsteady impeller-diffuser interaction in a transonic centrifugal compressor stage*, ASME Turbo Expo 2010, ASME Paper GT2010-22737 (2010)
13. K. Yamada, M. Furukawa, H. Arai, D. Kanazaki, *Evolution of Reverse Flow in a Transonic Centrifugal Compressor at Near-surge*, Proceedings of ASME Turbo Expo 2017, GT2017-63568 (2017)
14. T. Ceyrowsky, A. Hildebrandt, R. Schwarze, *Numerical investigation of the circumferential pressure distortion induced by a centrifugal compressor's external volute*, ASME Turbo Expo 2018, ASME paper GT2018-75919 (2018)
15. C. Rodgers, *Centrifugal Compressor Inlet Guide Vanes for Increased Surge Margin*, J. Turbomach., 113, 696–702 (1991)
16. M. Ishida, D. Sakaguchi, H. Ueki, *Effect of Pre-Swirl on Unstable Flow Suppression in a Centrifugal Impeller with Ring Groove Arrangement*, In Proceedings of the ASME Turbo Expo: Power for Land, Sea, and Air, Barcelona, Spain, 8–11 May 2006, GT2006-90400. p. 90400 (2006)
17. B. Nikpour, *Turbocharger Compressor Flow Range Improvement for Future Heavy Duty Diesel Engines*, In Proceedings of the THIESEL 2004 Conference on Thermo- and Fluid Dynamic Processes in Diesel Engines, 7–10 September 2004, Valencia, Spain, (2004)
18. J. Xiao, W. Xu, C. Gu, X. Shu, *Self-recirculating casing treatment for a radial compressor*, Chin. J. Mech. Eng., 22, 567–573 (2009)
19. S. Sivagnanasundaram, S. Spence, J. Early, B. Nikpour, *An impact of Various Shroud Bleed Slot configurations and Cavity Vanes on Compressor Map Width and the Inducer Flow Field*, J. Turbomach., 135, 041003 (2013)

20. N. Yamaguchi, *The Development of Effective Casing Treatment for Turbocharger Compressors*, In Proceedings of the IMechE Seventh International Conference, 14–15 May 2002, London, UK (2002)
21. H. Tamaki, *Effect of Recirculation Device on Performance of High-Pressure Ratio Centrifugal Compressor*, In Proceedings of the Turbo Expo: Power for Land, Sea, and Air, Glasgow, UK, 14–18 June 2010, Volume 44021, pp. 1879–1889 (2010)
22. H. Tamaki, *Effect of recirculation device with counter swirl vane on performance of high-pressure ratio centrifugal compressor*, J. Turbomach., 134, 051036 (2012)
23. P. X. L. Harley, A. Starke, T. Bamba, D. Filsinger, *Axial groove casing treatment in an automotive turbocharger centrifugal compressor*, Proceedings of the Institution of Mechanical Engineers, Part C: Journal of Mechanical Engineering Science, 232, 24, 4472-4484 (2018)
24. S. Leichtfuß, J. Bühler, H. P. Schiffer, P. Peters, M. Hanna, *A Casing Treatment with Axial Grooves for Centrifugal Compressors*, International Journal of Turbomachinery, Propulsion and Power, 4, 3, 27 (2019)
25. P. Gao, Y. Zhang, S. Zhang, *Numerical investigation of the different casing treatment in a centrifugal compressor*, In 2010 Asia-Pacific conference on wearable computing systems, pp. 51-54, IEEE (2010)
26. X. Chen, Z. Ai, Y. Ji, G. Qin, *Numerical investigation of a centrifugal compressor with a single circumferential groove in different types of diffusers*, In Turbo Expo: Power for Land, Sea, and Air, Vol. 50800, p. V02CT44A004 (2017)
27. C. Cravero, *A design methodology for radial turbomachinery. Application to turbines and compressors*, The 2002 Joint US ASME European Fluid Engineering Summer Conference paper FEDSM2002 31335, 14-18 July 2002, Montreal (2002)
28. M. Bardelli, C. Cravero, M. Marini, D. Marsano, O. Milingi, *Numerical Investigation of Impeller-Vaned Diffuser Interaction in a Centrifugal Compressor*, Appl. Sci., 9, 1619 (2019)
29. M. Carretta, C. Cravero, D. Marsano, *Numerical Prediction of Centrifugal Compressor Stability Limit*, In Proceedings of the ASME Turbo Expo: Turbomachinery Technical Conference and Exposition, Charlotte, NC, USA, 26–30 June 2017, Paper GT2017-63352 (2017)
30. C. Cravero, D. Marsano, *Criteria for the Stability Limit Prediction of High-Speed Centrifugal Compressors with Vaneless Diffuser. Part I: Flow Structure Analysis*, In Proceedings of the ASME Turbo Expo 2020: Turbomachinery Technical Conference and Exposition, Online, 21–25 September 2020; Paper GT2020-14579 (2020)
31. C. Cravero, D. Marsano, *Criteria for the Stability Limit Prediction of High-Speed Centrifugal Compressors with Vaneless Diffuser. Part II: The development of Prediction Criteria*, In Proceedings of the ASME Turbo Expo 2020: Turbomachinery Technical Conference and Exposition, Online, 21–25 September 2020; Paper GT2020-14589 (2020)
32. C. Cravero, P. J. Leutcha, D. Marsano, *Simulation and modelling of ported shroud effects on radial compressor stage stability limits*, Energies, Vol. 15, 7, p. 2571 (2022)
33. C. Cravero, D. Marsano, V. Sishtla, C. Halbe, W. T. Cousins, *Numerical investigations of near surge operating conditions in a two-stage radial compressor with refrigerant gas*, In Proceedings of the ASME Turbo Expo 2023: Turbomachinery Technical Conference and Exposition, Boston, Massachussets, USA, 26–30 June 2023; Paper GT2023-102630 (2023)

34. C. Cravero, D. Marsano, *Numerical prediction of tonal noise in centrifugal blowers*, In Turbo Expo: Power for Land, Sea, and Air, Vol. 50985, p. V001T09A001 (2018)
35. P. Silvestri, S. Marelli, M. Capobianco, *Incipient Surge Analysis in Time and Frequency Domain for Centrifugal Compressors*, Journal of Engineering for Gas Turbines and Power, Vol. 143, 10, art. No. 101020 (2021)
36. C. A. N. M. D. H. Champ, P. Silvestri, M. L. Ferrari, A. F. Massardo, *Incipient Surge Detection in Large Volume Energy Systems Based on Wigner–Ville Distribution Evaluated on Vibration Signals*, Journal of Engineering for Gas Turbines and Power, Vol. 143, 7, art. no. 071014 (2021)
37. F. Reggio, P. Silvestri, M. L. Ferrari, A. F. Massardo, *Operation extension in gas turbine-based advanced cycles with a surge prevention tool*, Meccanica, Vol. 57, 8, pp. 2117-2130 (2022)